Toughened Polyoxymethylene by Polyolefin Elastomer and Glycidyl Methacrylate Grafted High Density Polyethylene

Wenqing Yang,[1] Xuan-Lun Wang,[1] Xingru Yan,[2] Zhanhu Guo[2]
[1] *College of Materials Science and Engineering, Chongqing University of Technology, Chongqing 400054 People's Republic of China*
[2] *Integrated Composites Laboratory (ICL), Department of Chemical & Biomolecular Engineering University of Tennessee, Knoxville, Tennessee 37997*

Ternary blends of polyoxymethylene (POM), polyolefin elastomer (POE), and glycidyl methacrylate grafted high density polyethylene (GMA-g-HDPE) with various component ratios were studied for their mechanical and thermal properties. The size of POE dispersed phase increased with increasing the elastomer content due to the observed agglomeration. The notched impact strength demonstrated a parabolic tendency with increasing the elastomer content and reached the peak value of 10.81 kJ/m^2 when the elastomer addition was 7.5 wt%. The disappearance of epoxy functional groups in the POM/POE/GMA-g-HDPE blends indicated that GMA-g-HDPE reacted with the terminal hydroxyl groups of POM and formed a new graft copolymer. Higher thermal stability was observed in the modified POM. Both storage modulus and loss modulus decreased from dynamic mechanical analysis tests while the loss factor increased with increasing the elastomer content. GMA-g-HDPE showed good compatibility between the POM matrix and the POE dispersed phase due to the reactive compatibilization of the epoxy groups of GMA and the terminal hydroxyl groups of POM. A POM/POE blend without compatibilizer was researched for comparison, it was found that the properties of P-7.5(POM/POE 92.5 wt%/7.5 wt%) were worse than those of the blend with the GMA-g-HDPE compatibilizer. POLYM. ENG. SCI., 00:000–000, 2017.

INTRODUCTION

Polyoxymethylene (POM), an excellent engineering plastic with high stiffness, excellent flexural modulus and tensile strength, and good chemical resistance, has shown extensive applications including automobiles, electronic industry, mechanical industry, constructions and so on [1–4]. Due to its high degree of crystallinity of about 70%, POM exhibits poor impact strength [4, 5]. Many additives have been reported to improve the impact strength of POM. For example, thermoplastic polyurethane (TPU) as an excellent elastomer was reported to possess compatibility with POM due to the effect of hydrogen bonds [6]. The TPU modified POM has been researched extensively [7–12]. However, TPU is expensive, other elastomers are sought to modify POM. For example, Pan et al. [13] prepared toughened POM with gel acrylonitrile–butadiene elastomer (GNBE), in which system the phenol formaldehyde resin (PFR) acted as compatibilizer, the notch impact strength of the blend POM/GNBE (80/20) with 6 phr PFR reached 21.6 kJ/m^2, 248.4% higher than pure POM (6.2 kJ/m^2), the elongation at break was 133%, 323.6% higher than pure POM (31.4%), and the tensile strength was 33.8 MPa, 41.1% lower than pure POM (57.4MPa). Polyolefin elastomer (POE) is an excellent elastomer and can be used to toughen the thermoplastics by blending. For example, Svoboda et al. [14] blended PP and ethylene–octene copolymer (EOC) with different proportions to investigate their elastic properties. The elongation at break of pure EOC was 860%, decreased to 316% with 40% PP (elongation at break of pure PP was 425%), and was reduced sharply to 5% with further adding PP due to the poor compatibility of these two components. Significant disparity between POM and POE was observed leading to incompatibility in the POM/POE blends. Uthaman et al. [15] blended POM with EOC, and reported that the notch impact was decreased from 70.09 to 49.12 J/m with increasing the EOC content from 0 wt% to 20 wt%.

Compatibilizer is very important in modifying plastics as it acts as the role of bridging different ingredients together. For example, Wildes et al. [16] studied an amine-functional styrene–acrylonitrile (SAN–amine) polymer as the reactive compatibilizer in the polycarbonate/acrylonitrile butadiene styrene (PC/ABS) blends, the synthetic copolymer compatibilizer offered excellent stability for the blends. Lertwimolnun and Vergnes [17] fabricated the PP/organoclay nanocomposites, in which system the PP grafted with maleic anhydride (PP-g-MA) was used to promote the clay distribution. Kim et al. [18] blended PP and ethylene vinyl alcohol (EVOH) with and without 10 wt% compatibilizer polypropylene grafted with itaconic acid (PP-g-IA), SEM pictures showed that PP and EVOH blended more uniformly with PP-g-IA than PP/EVOH blends without PP-g-IA, and there was no obvious "sea-island" structure in the PP/EVOH/PP-g-IA blends. Bettini et al. [19] prepared PP/coir fiber (CF) composites, and incorporated PP-g-MA as compatibilizer, SEM micrographs indicated that PP and CF contacted closer with PP-g-MA than the blends PP/CF without PP-g-MA. Zhao et al. [20] blended polylactic acid (PLA)/poly ε-Caprolactone) (PCL) to study the rheological properties of the blends and showed that when the PCL content increased (less than 30%), the storage modulus increased because of entanglements of the polymer chains.

Glycidyl methacrylate (GMA) can be used to improve compatibility and thermal stability of the thermoplastics. For example, Su et al. [21] studied the morphology and properties of PLA/GMA-g-POE, and reported a partial compatibility between these two components due to the reaction between epoxy groups

Correspondence to: X.-L. Wang; e-mail: wangxuanlun@cqut.edu.cn or Z. Guo; e-mail: nanomaterials2000@gmail.com, zguo10@utk.edu
Contract grant sponsor: Chongqing Municipal Key Laboratory of Institutions of Higher Education for Mould Technology; contract grant number: MT201507.
DOI 10.1002/pen.24489
Published online in Wiley Online Library (wileyonlinelibrary.com).

from GMA and carboxyl groups from PLA. The epoxy groups from GMA can also react with hydroxyl end groups of polyester, GMA copolymer acted as reactive compatibilizer, the reaction was reported as follows [22–25]. As a copolymer-type, polyoxymethylene has terminal groups of $-CH_2-OH$ [1], it is supposed that GMA may react with hydroxyl end groups of POM for a good compatibility. However, the usage of glycidyl methacrylate grafted high density polyethylene (GMA-g-HDPE) for the POM and POE blend has not been reported.

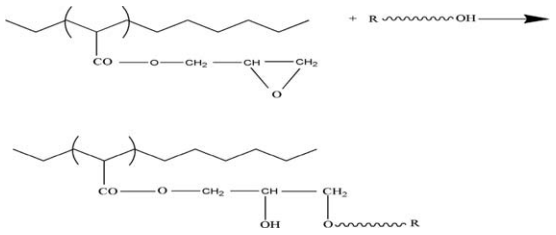

(R is the backbone of polyester)

In this work, GMA-g-HDPE was applied as the reactive compatibilizer of POM/POE blends to improve the toughness of POM. The component ratio was varied in the ternary blend system. The compatibility, morphology, mechanical and thermal properties of the ternary blends were investigated with scanning electron microscope (SEM), dynamic mechanical analysis (DMA), differential scanning calorimetry (DSC), and thermogravimetry analysis (TGA).

EXPERIMENTAL

Materials

Polyoxymethylene copolymer (M90, commercial grade, MI: 9, M_w: 1.69×10^5, PDI:2.84) was obtained by Yunnan Yuntianhua Co., Ltd, China. Polyolefin elastomer (POE VM6202 MI: 7.4, melting point: 61.56°C, M_w: 2×10^6, PDI:1.32) was purchased from Exxon Mobil Corporation. The compatibilizer GMA-g-HDPE (TRD-G400H, density 0.946 g/cm^3, MI: 0.5–4.0, grafting ratio 0.8–1.2 wt%, M_w: 8.47×10^5, PDI:6.5) was purchased from Shared Plastic Co., LTD, Yang Zhou China. Antioxidant 1010 was purchased from BASF Company.

Fabrication of Toughened Polyoxymethylene Alloys

Before extrusion process, pure POM was dried at 80°C in a precise drying oven (Blue Pard, BPG-9070A, China) for 3 h, POE and GMA-g-HDPE at 50°C for 3 h. The ternary blends of POM/POE/GMA-g-HDPE were prepared with various proportions with a co-rotating twin screw extruder (TSE-30A, L/D: 40:1, Nanjing Ruiya First Polymer Processing Equipment Co., LTD, China), and the temperatures of the extruder from feed aperture section to extrusion die were 115, 130, 170, 190, 195, 195, 195, 195, 195, and 190°C, respectively, with a screw speed of 200 rpm. A granulator was used to prepare granules. Then the granules were dried. The injection-molded process was inducted by an injection molding facility (EM80-SVP/2, Zhen-Xiong Co., Taiwan), and temperatures from feed aperture section to nozzle was 20, 165, 185, 190, and 185°C, respectively, injecting pressure was 120 MPa. Through every injection-molded process, a dumbbell-shaped sample for tensile test and a rectangle sample (80 mm × 10 mm × 4 mm) with a B-type notch (the depth was 2 mm) was obtained (two-cavity mold). For the sake of clarity, the experimental formulation is summarized in Table 1. The total mass of POM and POE was regarded as 100 wt%, the mass of compatibilizer, i.e. GMA-g-HDPE, was half of POE, and the mass of antioxidant was 0.5 wt% to the total weight of POM and POE, respectively.

TABLE 1. Experimental formulation.

Sample code	POM (%)	POE (%)	GMA-g-HDPE (%)	Antioxidant (%)
POM	100	0	0	0
P-2.5C	97.5	2.5	1.25	0.5
P-5C	95	5	2.5	0.5
P-7.5C	92.5	7.5	3.75	0.5
P-10C	90	10	5	0.5
P-12.5C	87.5	12.5	6.25	0.5
P-15C	85	15	7.5	0.5
P-7.5	92.5	7.5	0	0.5

Characterization

The morphology was tested by a scanning electron microscopy (SEM JSM-6460LV, JEOL, Japan). The samples were prepared by fracturing at liquid nitrogen temperature. After that, the fractured surfaces were sputtered with a thin layer of gold for better imaging. To study the effect of compatibilizer on the tensile property, the tensile fracture surfaces of some samples were also sputtered with a thin layer of gold for better imaging. The voltage was 20 kV.

The tensile tests were conducted with an electromechanical universal testing machine (SANS, CMT 6104, MTS systems Co. Ltd, China) based on ASTM D638-10. The gauge length was 50 mm. The gauge rate was 50 mm/min. The notched izod impact strength was tested with a cantilever impact testing machine (JinJian XJU-5.5, China) based on ASTM D256-10. The model of pendulum bob was 2.75 J. Five samples were measured for each component when the tensile tests and impact tests were operated. All the tests were conducted at 25°C.

For the Fourier Transform infrared spectroscopy (FTIR) test, GMA-g-HDPE and P-7.5C were compressed into thin films by a tablet press (BL-6170-A, Bolon Precision Testing Machines Co., LTD), the molding temperature was 185°C, and then the thin films were measured in a Fourier transform infrared Spectrum instrument (Nicolet iS10 Documentation, Thermo Fisher Scientific). Number of scan was 32, resolution was 2 cm^{-1}.

The crystallization properties were characterized by differential scanning calorimetry (DSC, Q20, TA Instruments). The DSC measurements were conducted under nitrogen atmosphere. The flow rate of nitrogen was 50 mL/min. The samples about 5 mg were heated from 40 to 200°C by 10°C/min, and then maintained isothermally for 5 min to eliminate the heat history effect, then cooled down to 40°C at 10°C/min.

The thermal stability was operated with a thermogravimetric analysis (Q50, TA Instruments). The samples about 5 mg were heated from 25 to 600°C at 10°C/min under nitrogen atmosphere to observe their degradation behavior. The flow rate of nitrogen was 60 mL/min. The onset temperature of degradation was regarded as the temperature when the loss weight was 5 wt%.

The viscoelastic behavior of the blends was studied with a dynamic mechanical analysis (DMA, Q800, TA Instruments).

DOI 10.1002/pen

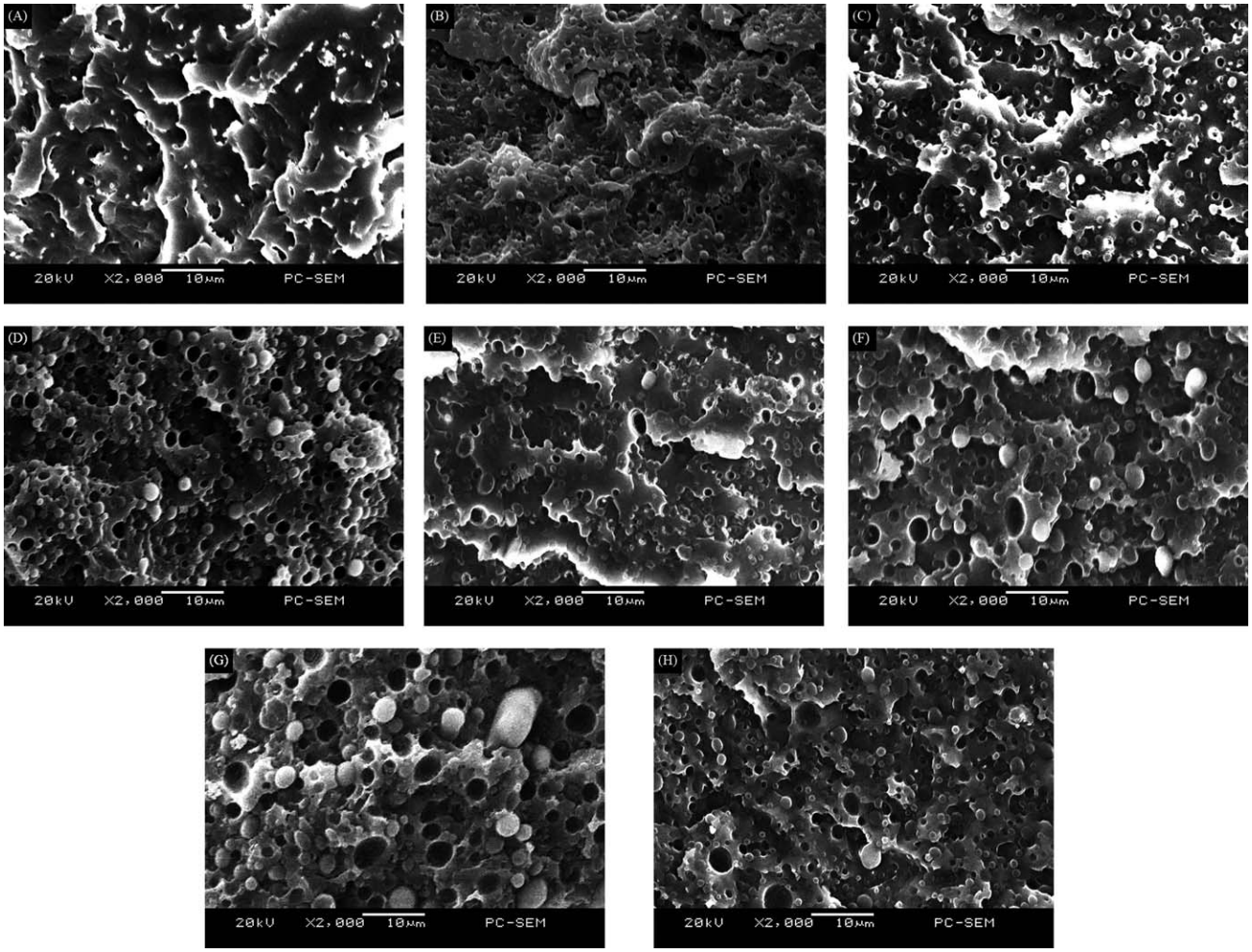

FIG. 1. SEM micrographs of the cryo-fractured surface of (A) POM; (B) P-2.5C; (C) P-5C; (D) P-7.5C; (E) P-10C; (F) P-12.5C; (G) P-15C; and (H) P-7.5.

The dimensions of the samples were about 35 mm × 10 mm × 4 mm. The testing mode was DMA Multi-Frequency-Strain, POM and toughened POM blends were heated from −90 to 150°C, by 3°C/min under 10 Hz load (single frequency), the amplitude was 10 μm, POE was heated from −90 to 55°C (The melting point of POE is 61.56°C), by 3°C/min under 10Hz (single frequency), the amplitude was 10 μm.

RESULTS AND DISCUSSION

Morphologies of the Fractured Surfaces

Figure 1 shows the fractured surface morphology of the samples while Table 2 shows the POM particle numbers and average diameters in the POM matrix analyzed by Image-Pro Plus 6.0 software in the figures. Pure POM is a brittle material, when broken in nitrogen temperature, it created debris. When POM was blended with POE, the distributed POE particles in POM matrix absorbed energy by deformation, thus the toughness of materials was increased when the POM/POE blends were broken. The appearance of the POE dispersed phase was spherical or columnar. The size of the dispersed phase increased as the content of elastomer increased. When the loading of POE was 15 wt%, the size of the dispersed phase was the largest. The particle number increased with increasing the elastomer content from 0 to 7.5 wt%, the particle number reached the maximum at 7.5 wt% content. Meanwhile, the decreased inter-particle distance lead to an increase in the impact strength. The sharp brittle-tough transition would take place at a critical inter-particle distance when the content of elastomer was relatively high. At lower content of elastomer, the particles dispersed uniformly, and the diameter of particles was similar. At higher content of elastomer, when the content of elastomer increased, the particle size increased and the number of particles decreased due to agglomeration. The interface between particles and matrix was blurry arising from the enhanced compatibility

TABLE 2. POE particle distribution in POM matrix.

Sample Test item	P-2.5C	P-5C	P-7.5C	P-10C	P-12.5C	P-15C	P-7.5
Particle numbers	280	306	410	304	232	160	394
Average diameter (μm)	0.75	1.32	1.64	1.85	2.07	3.64	1.73

TABLE 3. Mechanical properties of pure P-7.5 and POE.

Codes	σ_M[a]	ε_B[b]	izod[c]	E[d]
P-7.5	51.31	47.82	9.31	1,728
POE	3.65	1,358		55

[a]Tensile strength (MPa).
[b]Elongation at break (%).
[c]Notched izod impact strength (kJ/m^2).
[d]E is tensile modulus (MPa).

between the POM matrix and the POE dispersed phase brought by the GMA-g-HDPE. On the other hand, compared with P-7.5C, very serious agglomeration and broad particle size distribution were observed in the fracture surface of P-7.5, the particle number of P-7.5 was relatively lower than P-7.5C, and the particle average diameter was a little higher than that of P-7.5C, this also demonstrated that the compatibilizer was necessary for obtaining high quality of POM/POE blends.

Mechanical Properties

The tensile strength, elongation at break, notch impact strength and tensile modulus of pure POM, POE and their blends are showed in Table 3 and Figure 2. The notched impact strength was improved with the addition of POE elastomer. A peak value of the notched impact strength was observed with

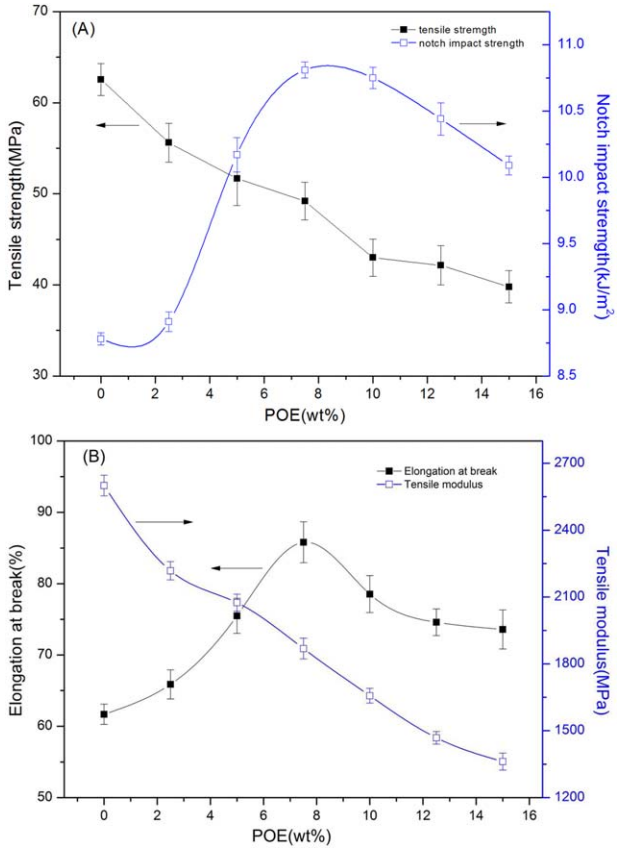

FIG. 2. (A) Tensile strength and Notch impact strength (B) Elongation at break and Tensile modulus vs POE (wt%) of POM and compatibilized POM/POE/GMA-g-HDPE (Note: when POE (wt%) was 0, the material was POM). [Color figure can be viewed at wileyonlinelibrary.com]

increasing the elastomer content. From 0 to 7.5 wt%, the notch impact strength was increased positively related to the POE elastomer. At 7.5 wt%, the notch impact strength reached 10.81 kJ/m^2, increased by 23.1% than that of pure POM (8.78 kJ/m^2), due to the increased interfacial adhesion between matrix and dispersion phase in the presence of the compatibilizer [26]. The GMA possesses good compatibility with POM matrix with the epoxy groups of GMA being reacted with terminal hydroxyls of POM to form a new grafting copolymer. In addition, GMA-g-HDPE and POE are compatible because both have polyolefin main chain structures. When the samples were subjected to an impact, the energy passed from POM matrix to POE elastomer via interface, the POE elastomer would absorb impact energy by elongation transformation as its elongation at break was as high as 1,358%, and thus the impact strength of POM/POE blends was improved. With further increasing the POE elastomer content, the notched impact strength suffered a downward trend. When the addition was 15 wt%, the notched impact strength dropped down to 10.09 kJ/m^2, but still higher than that (8.78 kJ/m^2) of pure POM by 14.9%. The reason for the decreased notched impact strength was due to the elastomer agglomeration (as verified by the SEM) when its dosage was above 7.5 wt%, the agglomeration of elastomer decreased both the number of elastomer particles and the interface between the matrix and dispersed phase. The elongation at break was another important parameter of toughness, the same trend as the notch impact strength was observed. The elongation at break of POE was 1,358%, much higher than that of pure POM (61.68%), at 0–7.5 wt% addition of POE elastomer, the elongation at break was increased, and reached a maximum 85.81%, 39.1% higher than that of pure POM. Then the value decreased to 73.58% with further increasing the POE elastomer loading to 15 wt%. Generally, the improved impact performance by elastomer always means a sacrifice of the tensile strength [27]. The tensile strength of POE was 3.65 MPa, much lower than that of pure POM (62.56 MPa), with increasing the elastomer loading, the tensile strength of the samples decreased due to the lower tensile strength of elastomer. The tensile strength decreased steadily with increasing the POE elastomer content. With 7.5 wt% addition, the tensile strength was 49.21 MPa, 21.3% lower than that of pure POM. In addition, the notch impact strength of P-7.5 (without any compatibilizer) was 9.31 kJ/m^2, lower than that of P-7.5C (10.81 kJ/m^2), attributed to serious agglomeration and broad particle size distribution, as verified by the SEM observation.

Tensile fracture surface of P-7.5C and P-7.5 was shown in Figure 3. Apparently, the tensile fracture surface of P-7.5C was much rougher than P-7.5, indicating that the tensile toughness of P-7.5C was better than P-7.5 in the presence of compatibilizer.

Infrared Spectroscopic Analysis

Figure 4 shows the FTIR spectra of GMA-g-HDPE, P-7.5C and P-7.5 and Figure 5 shows a zoomed view of Figure 4 in the range of 600–950 cm^{-1} Apparently, the GMA-g-HDPE has epoxy functional groups as shown by the peaks at around 841, and 900 cm^{-1} [28], Figure 5a. However, no epoxy functional groups were observed at 841 and 900 cm^{-1} in the P-7.5C sample, Figure 5b. As the epoxy functional groups could only react with the terminal hydroxyl groups of POM in the formula POM/

DOI 10.1002/pen

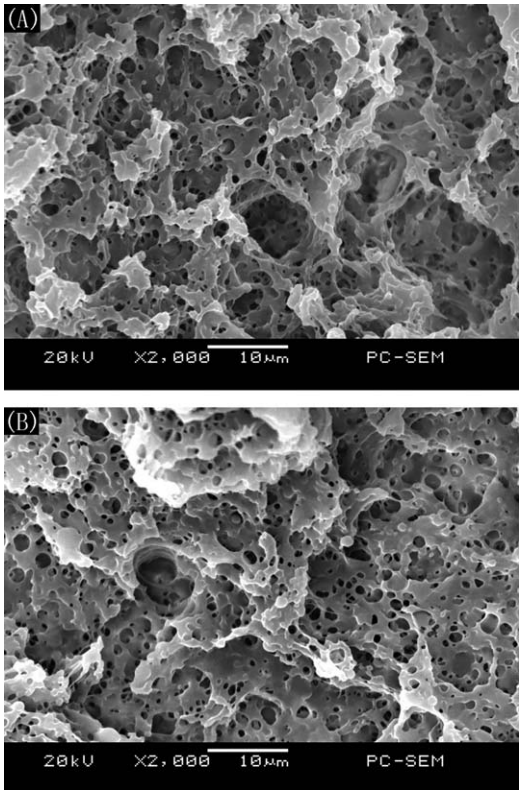

FIG. 3. Tensile fracture surface of (A) P-7.5C and (B) P-7.5.

POE/GMA-g-HDPE. This confirmed that GMA-g-HDPE had reacted with POM and formed a new graft copolymer; chemical equation is shown as follows [22–25]:

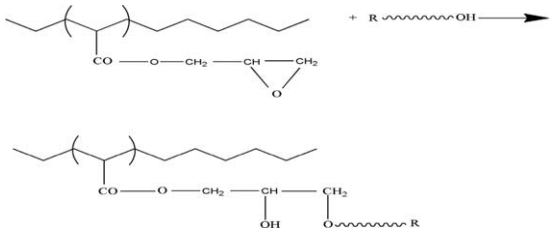

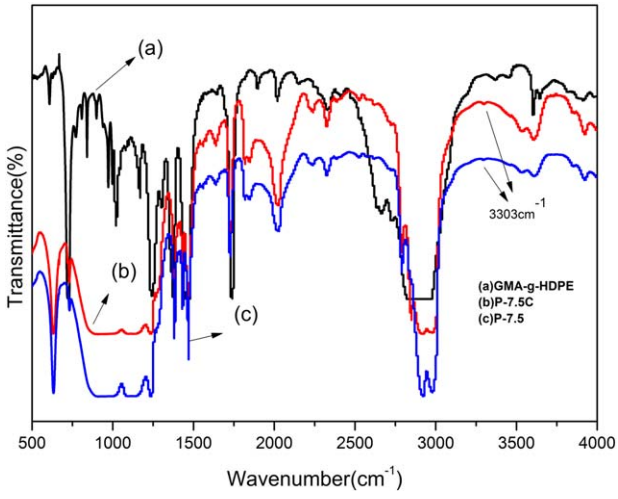

FIG. 4. FTIR spectra of (a) GMA-g-HDPE, (b) P-7.5C, and (c) P-7.5. [Color figure can be viewed at wileyonlinelibrary.com]

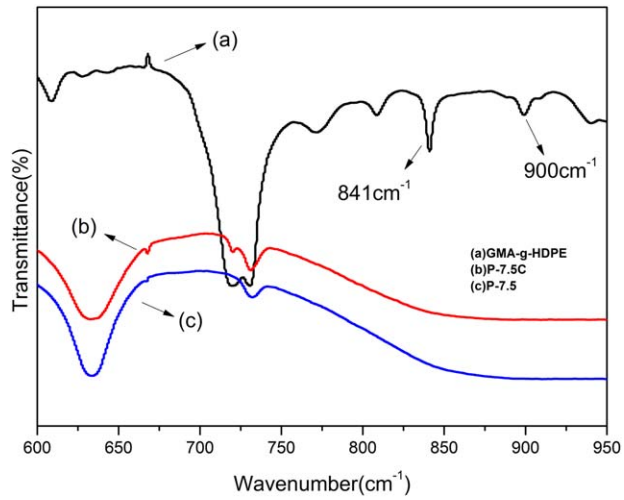

FIG. 5. Zoomed view of Figure 4 in the range of 600–950 cm^{-1}. [Color figure can be viewed at wileyonlinelibrary.com]

This confirms that GMA-g-HDPE is an excellent compatibilizer as it can react with POM and also can have good compatibility with POE because both have polyolefin backbone structure.

P-7.5 (without compatibilizer) has primary alcohol hydroxyl. In P-7.5C, the primary alcohol hydroxyl reacted with epoxy group, and generated secondary alcohol hydroxyl. Primary alcohol hydroxyl absorbance was at 3,303 cm^{-1}, this could also be observed from Figure 4b. There was also an absorbance at 3,303 cm^{-1} from Figure 4c, as primary alcohol hydroxyl and secondary alcohol hydroxyl had almost the same absorbance, This confirms that the absorbance at 3,303 cm^{-1} from Figure 4c spectra was secondary alcohol hydroxyl generated by the reaction. Thus, GMA-g-HDPE was proved to be a reactive compatibilizer in the POM/POE/GMA-g-HDPE blends, and had good compatibility with POM. The mass fraction of POM in P-7.5C was lower than the mass fraction of POM in P-7.5, so the transmittance of P-7.5C was a little higher than P-7.5.

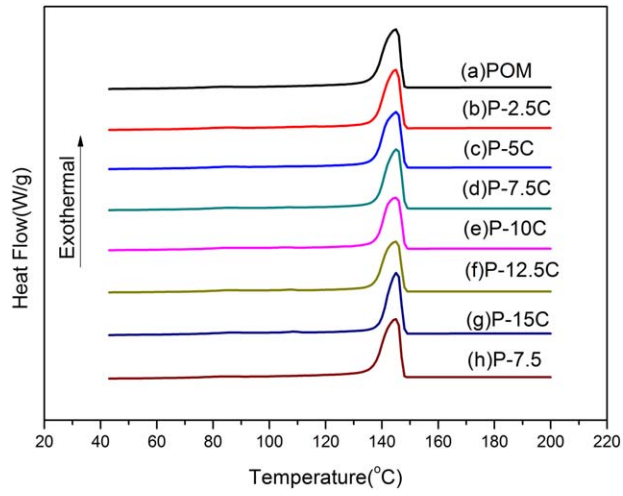

FIG. 6. DSC curves of (a) POM, (b) P-2.5C, (c) P-5C, (d) P-7.5C, (e) P-10C, (f) P-12.5C, (g) P-15C, and (h) P-7.5. [Color figure can be viewed at wileyonlinelibrary.com]

TABLE 4. Crystallization parameters for the POM-based blends.

Codes	ΔH_m(J/g)	F_C (%)
POM	143.8	75.68
P-2.5C	135.8	74.59
P-5C	130.6	74.52
P-7.5C	124.3	73.73
P-10C	119.85	73.94
P-12.5C	115.79	74.35
P-15C	111.95	74.87
P-7.5	131.6	75.24

ΔH_m is enthalpy change of crystallization, F_C is crystallinity calculated by weight.

Crystallization Properties and Thermal Stability

Figure 6 showed the DSC curves of pure POM, P-2.5C, P-5C, P-7.5C, P-10C, P-12.5C, and P-15C. The POM crystalline fraction (F_c) in the blend system was calculated based on *Equation 1* [29].

$$F_c = \Delta H_m / [\Delta H_m^o (1-x)] \quad (1)$$

where ΔH_m is the heat enthalpy of the samples, x is total mass percent of POE, GMA-g-HDPE and antioxidant in the blends, ΔH_m^o (190 J/g) is the heat enthalpy of pure POM with a complete crystallization [30].

The onset temperature of the crystallization and melting temperature of the samples were about 148 and 145°C, respectively. The results indicate that the crystal structure remained unchanged with the incorporation of elastomer and compatibilizer. The crystallinity of POM/POE blends decreased from 75.68% (POM) to 73.73% for P-7.5C firstly and then increased to 74.87% for P-15C. All the POM/POE blends had a lower crystallinity than pure POM, as shown in Table 4. That was because the chain segments were adhered to the interface in the form of amorphous state, as the gross chain segments were constant, fewer POM chain segments entered into the crystals, i.e. the crystallinity of POM blends would be decreased than that of pure POM. From the following SEM microstructures, at lower dosage (0–7.5 wt%) of elastomer, the interfacial area of POM and POE increased with increasing the content of elastomer, thus the crystallinity of POM blends decreased. When the dosage of elastomer was over 7.5 wt%, the interfacial area decreased relatively with increasing the content of elastomer because the elastomer was agglomerated, thus the crystallinity of POM blends increased. Besides, the crystallinity of P-7.5 was 75.24%, only a little lower than that of pure POM (75.68%). This was because without compatibilizer, the interface adhesion was weak, fewer POM molecule segments were adhered to the interface in the form of amorphous state.

Thermal Stability

Figure 7 shows the thermal stability behavior of pure POM, POE and their blends. Obviously, pure POM and POE exhibited a one-step degradation while their blends showed a two-step degradation. In the degradation process, the POM matrix was degraded firstly and then the degradation of the dispersed phase of POE was observed. In the first step, the onset degradation

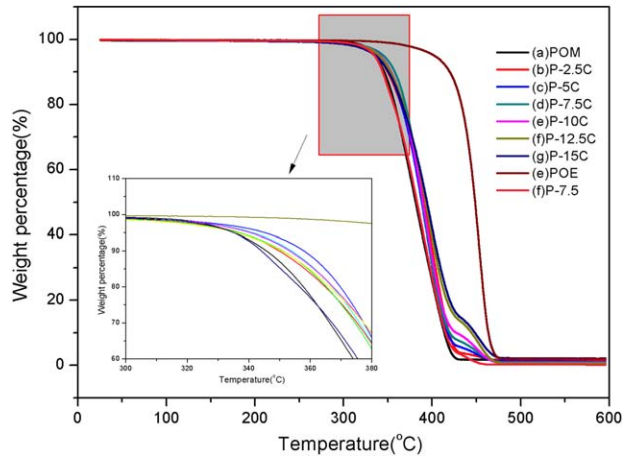

FIG. 7. TGA curves of POM, POE, P-7.5, and their compatibilized blends. [Color figure can be viewed at wileyonlinelibrary.com]

temperature of POE was 410.06°C, higher than that of pure POM. For pure POM, the structure of main chains was —CH_2—O—, which was transferred to formaldehyde when the thermal decomposition began [30]. This would accelerate the degradation of POM. The improved onset degradation temperatures of POM/POE blends compared with pure POM are also shown in Figure 7. The onset degradation temperature of the blends showed a parabolic tendency with increasing the elastomer content. At lower dosage of elastomer, the interface between POE and POM increased when the elastomer loading increased, more POM segments were adhered to the POE particles, which had a higher degradation temperature and higher viscosity, thus the mobility of the POM segments decreased and the degradation temperature of POM phase increased. While at a higher dosage of elastomer, the interfacial area decreased when the elastomer content increased because of the agglomeration of elastomer, so fewer POM segments were adhered to the POE particles, thus the degradation temperature of POM phase decreased. The onset degradation temperatures (T_o) of the samples are listed in Table 5. At 7.5 wt% addition of elastomer, this onset degradation temperature reached a peak value of 347.24°C, 12.86°C higher than that of pure POM. This was attributed to the reactive compatibility between POM and GMA-g-HDPE compatibilizer, in consistence with the fact that the impact strength reached the peak value at 7.5 wt% elastomer. The second degradation temperature of the blends was similar to that of pure POE, this indicated that the component of POE did not have an obvious chemical reaction with GMA-g-

TABLE 5. Onset degradation temperatures (T_o) of the samples.

Codes	T_o (°C)
POM	334.38
P-2.5C	334.94
P-5C	338.60
P-7.5C	347.24
P-10C	337.48
P-12.5C	337.07
P-15C	336.89
P-7.5	335.08
POE	410.06

DOI 10.1002/pen

HDPE compatibilizer during the blending process. Furthermore, the onset degradation temperature of P-7.5 was 335.08°C, only a little higher than that of pure POM (334.38°C), much lower than that of P-7.5C (347.24°C), this was because of the weak interface adhesion without compatibilizer.

Dynamic Mechanical Properties

Figure 8A shows the storage modulus of POM, modified POM blends and POE (The melting point of POE is 61.56°C) as a function of temperature. The storage modulus of all the samples decreased with increasing the temperature, this was due to the increased chain segment mobility with increasing the temperature. The storage modulus of POE was much lower than that of POM, as Figure 9 showed. The modified samples possess a lower storage modulus than that of pure POM. The storage modulus was often associated with the "stiffness" of a polymeric material and was related to the elastic modulus [31]. The stiffness for a rectangular cross section sample was calculated as *Eq. 2* [32].

$$K = \frac{24EI}{L^3\left[1+12/5(1+v)\left(\frac{t}{L}\right)^2\right]} \quad (2)$$

where K is the stiffness or spring constant (N/m), E is the elastic modulus (equal to tensile modulus) (Pa), L is the sample length (one side, m), t is the sample thickness (m), I is the sample moment of inertia (m^4), and v is the Poison's ratio.

With increasing the POE loading, the stiffness of the POM/POE blends became lower. Figure 8B shows the loss modulus as a function of temperature. The dynamic loss modulus was often associated with the "internal friction" [33] and sensitive to different kinds of molecular motions, relaxation, transitions, morphology and other structural heterogeneities [34]. The loss modulus of POE was much lower than that of POM, and loss modulus showed a similar tendency to the storage modulus as the content of elastomer and compatibilizer increased above room temperature. The decreased loss modulus was also due to the improved compatibility. On the other hand, the loss modulus reached a peak value at about 110°C, and began to decrease at above 110°C due to the destroyed crystalline structure. ΔH_m is the enthalpy change of crystallization in the whole sample. A lower ΔH_m means that the crystals became fewer in the whole sample. In Table 4, ΔH_m became lower with increasing the content of POE elastomer. The loss modulus decreased with increasing the content of POE elastomer, Figure 8B. This indicated that loss modulus decreased with the crystals decreasing in the sample. Commonly, weak interfacial adhesion has a negligible effect on the neighboring chain motion. However, good interfacial adhesion significantly restricted the movement of the main chain segments. The result showed a good interfacial adhesion of the POM/POE/GMA-g-HDPE blends.

Furthermore, Komalan et al. blended nylon copolymer/EPDM rubber and EPM grafted maleic anhydride (EPM-g-MA) compatibilizer [35]. The addition of EPM-g-MA as compatibilizer improved the viscoelastic properties, indicating an improved interaction between these two components in the compatibilized system. EPM-g-MA improved the interfacial adhesion; consequently, the storage modulus of the blends was enhanced. As shown in Figure 8A and B, the storage modulus and loss

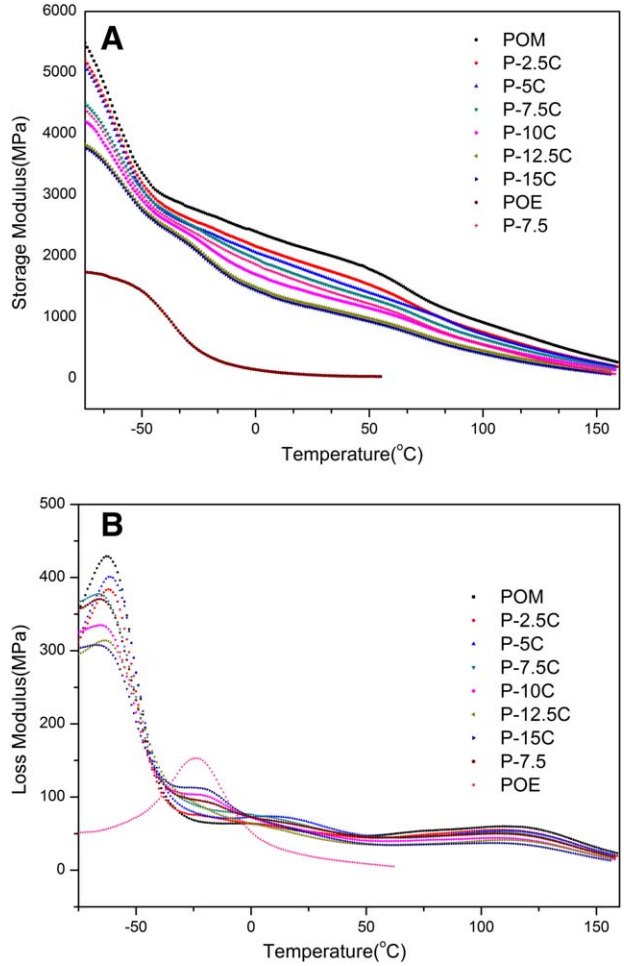

FIG. 8. (A) Storage modulus; and (B) Loss modulus of POM, modified POM blends and POE. [Color figure can be viewed at wileyonlinelibrary.com]

modulus of P-7.5C was higher than that of P-7.5, which reflected a better interfacial bonding due to the excellent compatibility between the POM matrix and the separation phase of POE due to the compatibilization of GMA-g-HDPE.

Figure 9 shows the loss factor as a function of temperature of POM, modified POM blends and POE. Apparently, the loss factor of POE was much higher than that of POM, so with increasing the content of elastomer and compatibilizer, the loss factor increased gradually. With 15 wt% addition of POE, the loss factor was the largest for all the measured temperature. The phenomena were due to the fact that POE as elastomer had a larger mechanical loss than pure POM. The loss factor increased with increasing the temperature, because the storage modulus of the blends decreased continuously while the loss modulus increased before the α relaxation (at around 125°C, the POM crystals began to melt). At higher temperatures, the chain segments began to move out of the POM crystals, leading to the increase in α relaxation. Furthermore, the broad single peak in each curve increased with increasing the elastomer and compatibilizer content, this was because the compatibility between the matrix and elastomer particles increased under the function of compatibilizer GMA-g-HDPE. Uthaman et al. [15] blended POM and POE with 0.1 wt% DCP, the impact strength was

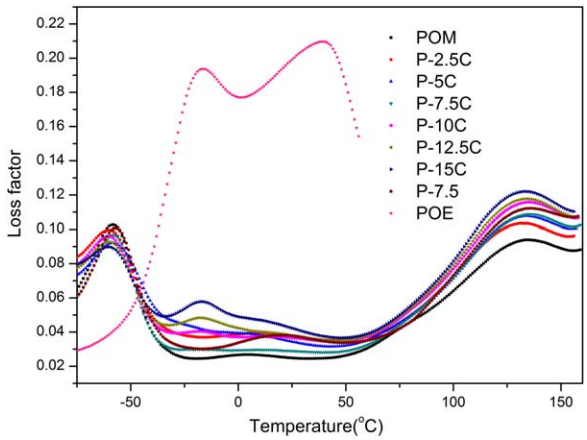

FIG. 9. Loss factor vs temperature of POM, modified POM blends and POE. [Color figure can be viewed at wileyonlinelibrary.com]

improved in the dynamic vulcanized system, the loss factor peak value of pure POM was about 0.083, and the loss factor of other blends with different proportions of ingredients was ranged from about 0.078 to 0.087. While in this research, the loss factor peak value was ranged from about 0.09 to 0.115. A higher loss factor means a more energy loss, and the materials with higher loss factor are more suitable to be used as damping parts. Moreover, the loss factor of P-7.5 was higher than that of P-7.5C, this was because of larger internal mechanical loss for the system without compatibilizer with a weak interface adhesion.

CONCLUSIONS

The mechanical, thermal properties and microstructures of the POM blends had been investigated. P-7.5C had the best performance as it exhibited the highest notched izod impact strength and highest thermal stability. Due to the reaction between the epoxy groups from GMA and the hydroxyl end groups from POM, the GMA-g-HDPE had good compatibility with POM matrix. P-7.5C had higher dynamic storage modulus than P-7.5, indicating that GMA-g-HDPE had good compatibility effect for POM/POE blends. The SEM micrographs showed that the POE particles existed in the state of spherical or columnar in POM matrix, and the interface between the POM matrix and POE particles increased firstly and then decreased. In addition, the fracture surface of P-7.5 proved that the particles were not distributed uniformly without compatibilizer.

REFERENCES AND CITED WORK

1. C.E. Carraher, *Giant Molecules: Essential Materials for Everyday Living and Problem Solving*, John Wiley & Sons, Hoboken, New Jersey, USA (2003).
2. L. Guo, X. Xu, Y. Zhang, and Z. Zhang, *Polym. Compos.*, **35**, 127 (2014).
3. R.N. Uthaman, A. Pandurangan, and S.S.M. Majeed, *Polym. Eng. Sci.*, **47**, 934 (2007).
4. A.K. Das, S. Suin, N.K. Shrivastava, S. Maiti, J.K. Mishra, and B.B. Khatua, *Polym. Compos.*, **35**, 273 (2014).
5. X.C. Ren, L. Chen, and H.J.J. Zhao, *Macromol. Sci. Phys.*, **46**, 411 (2007).
6. K. Pielichowski and A.J. Leszczynska, *Polym. Eng.*, **25**, 359 (2005).
7. F. C. Chang and M. Y. Yang, *Polym. Eng. Sci.*, **30**, 543 (1990).
8. M. Mehrabzadeh and D.J. Rezaie, *Appl. Polym. Sci.*, **84**, 2573 (2002).
9. X. Gao, C. Qu, Q. Zhang, Y. Peng, and Q. Fu, *Macromol. Mater. Eng.*, **289**, 41 (2004).
10. S. Siengchin, J. Karger-Kocsis, G.C. Psarras, and R.J. Thomann, *Appl. Polym. Sci.*, **110**, 1613 (2008).
11. K. Palanivelu, S. Balakrishnan, and P. Rengasamy, *Polym. Test.*, **19**, 75 (2000).
12. G. Kumar, N.R. Neelakantan, and N.J. Subramanian, *Mater. Sci.*, **30**, 1480 (1995).
13. G.Q. Pan, J.Y. Chen, and H.L. Li, *Plast. Rubber Compos.*, **36**, 291 (2007).
14. P. Svoboda, R. Theravalappil, and D. Svobodova, *Polym. Test.*, **29**, 742 (2010).
15. R.N. Uthaman, A. Pandurangan, and S.A.J. Majeed, *Polym. Res.*, **14**, 441 (2007).
16. G.S. Wildes, T. Harada, and H. Keskkula, *Polymer*, **40**, 3069 (1999).
17. W. Lertwimolnun and B. Vergnes, *Polymer*, **46**, 3462 (2005).
18. J.S. Kim, J.H. Jang, D.Y. Lim, Y.S. Lee, Y. Chang, and D.H. Kim, *Polym. Eng. Sci.*, in press, doi:10.1002/pen.24357.
19. S.H.P. Bettini, A.C. Biteli, and B.C. Bonse, A.d.A. Morandim-Giannetti, *Polym. Eng. Sci.*, **55**, 2050 (2015).
20. H. Zhao, X. Yan, G. Zhao, and Z. Guo, *Polym. Eng. Sci.*, **56**, 939 (2016).
21. Z. Su, Q. Li, and Y. Liu, *Eur. Polym. J.*, **45**, 2428 (2009).
22. P. Martin, J. Devaux, and R. Legras, *Polymer*, **42**, 2463 (2001).
23. Y.J. Sun, G.H. Hu, and M. Lambla, *Polymer*, **37**, 4119 (1996).
24. M. Penco, M.A. Pastorino, and E. Occhiello, *J. Appl. Polym. Sci.*, **57**, 329 (1995).
25. N.K. Kalfoglou, D.S. Skafidas, and J.K. Kallitsis, *Polymer*, **36**, 4453 (1995).
26. C. Komalan, K.E. George, P.A.S. Kumar, et al. *Express Polym. Lett.*, **1**, 641 (2007).
27. L.F. Ma, X.F. Wei, and Q. Zhang, *Mater. Des.*, **33**, 104 (2012).
28. P. Martin, J. Devaux, R. Legras, M. Van Gurp, and M. Van Duin, *Polymer*, **42**, 2463 (2001).
29. Q. He, T. Yuan, X. Zhang, Z. Luo, N. Haldolaarachchige, L. Sun, D.P. Young, S. Wei, and Z. Guo, *Macromolecules*, **46**, 2357 (2013).
30. S. Lüftl, V.M. Archodoulaki, and S. Seidler, *Polym. Degrad. Stab.*, **91**, 464 (2006).
31. T.A. Osswald, *Understanding Polymer Processing: Processes and Governing Equations*, Hanser Publishers, Cincinnati, Ohio, USA (2011).
32. Dynamic Mechanical Analyzer, Q Series™, Getting started guide, Revision F, TA Instruments, Cincinnati, Ohio, USA (2004).
33. X. Chen, S. Wei, A. Yadav, R. Patil, J. Zhu, R. Ximenes, L. Sun, and Z. Guo, *Macromol. Mater. Eng.*, **296**, 434 (2011).
34. J.D. Ferry, *Viscoelastic Properties of Polymers*, 2nd ed., John Wiley Interscience, Hoboken, New Jersey, USA (1970).
35. C. Komalan, K.E. George, and P.A.S. Kumar, *Express Polym. Lett.*, **1**, 641 (2007).